Sorption kinetics of polycyclic aromatic hydrocarbons removal using granular activated carbon: Intraparticle diffusion coefficients

C. Valderrama [a], X. Gamisans [a], X. de las Heras [a], A. Farrán [b], J.L. Cortina [b,*]

[a] *Department of Mining Engineering and Natural Resources, EPSEM, UPC, 08240 Manresa, Spain*
[b] *Department of Chemical Engineering, ETSEIB, Universitat Politècnica de Catalunya, Av. Diagonal 647, 08028 Barcelona, Spain*

Abstract

Granular activated carbon (GAC) was evaluated as a suitable sorbent for polycyclic aromatic hydrocarbons (PAHs) removal from aqueous solutions. For this purpose, kinetic measurements on the extraction of a family of six PAHs were taken. A morphology study was performed by means of a scanning electron microscopy (SEM) analysis of GAC samples. Analyses of the batch rate data for each PAH were carried out using two kinetic models: the homogenous particle diffusion model (HPDM) and the shell progressive model (SPM). The process was controlled by diffusion rate the solutes (PAHs) that penetrated the reacted layer at PAH concentrations in the range of 0.2–10 mg L^{-1}. The effective particle diffusion coefficients (D_{eff}) derived from the two models were determined from the batch rate data. The Weber and Morris intraparticle diffusion model made a double contribution to the surface and pore diffusivities in the sorption process. The D_{eff} values derived from both the HPMD and SPM equations varied from 1.1×10^{-13} to 6.0×10^{-14} m^2 s^{-1}.

The simplest model, the pore diffusion model, was applied first for data analysis. The model of the next level of complexity, the surface diffusion model, was applied in order to gain a deeper understanding of the diffusion process. This model is able to explain the data, and the apparent surface diffusivities are in the same order of magnitude as the values for the sorption of functionalized aromatic hydrocarbons (phenols and sulphonates) that are described in the literature.

© 2008 Elsevier B.V. All rights reserved.

Keywords: PAH; Sorption; Granular activated carbon (GAC); Kinetic study; Diffusion coefficients

1. Introduction

Discharges from coal mines, old gas works and wood preservative treatment sites have been identified as being responsible for many of the contamination problems involving high levels of polycyclic aromatic hydrocarbons (PAHs) in soils and groundwater. As a result, many of these facilities have been recognized as priority targets for decontamination, as is the case in Europe through the Megasites Programme or in the case of the USA through the National Priorities List of Superfund Sites Program [1,2].

The main remediation processes tested initially included the utilization of physical containment barriers and groundwater pump-and-treat methods [3,4]. PAHs are typically characterized by low water solubility and high octanol–water partitioning coefficients. It is understood that PAHs that accumulate in the subsurface sorb on the organic matter in aquifers. The time frame for remediation sites therefore depends on desorption rates. However, desorption rates are diffusion-limited, i.e. this process cannot be accelerated by increasing groundwater flow rates. It is therefore not surprising that groundwater remediation efforts based on pump-and-treat techniques have failed, particularly in cases in which strongly sorbing compounds such as PAHs are present.

More recently, air stripping, soil washing and Fenton oxidation have been evaluated [5–8]. However, due to their poor biochemical degradability, sorption-based elimination processes have been identified as alternatives to PAH removal as is the case of permeable reactive barriers (PRBs), which have been postulated as suitable technology for overcoming this problem [9,10]. The major advantage of such processes lies in the

Nomenclature

a_s	stoichiometric coefficient
a	Elovich model constant (g mg^{-1} min^{-1})
A, B and g $(0 < g < 1)$	constants of the Redlich–Peterson isotherm
b	Elovich model constant (g mg^{-1})
C	total concentration of sorbing species (M)
C_{Ao}	concentration of sorbing species A in bulk solution (M)
C_r	total concentration of both sorbing in the sorbent phase (M)
C_{so}	concentration of sorbing species at the bead's unreacted core (M)
D_e	diffusion coefficient in solid phase (m^2 s^{-1})
D_{eff}	effective diffusion coefficient (m^2 s^{-1})
D_m	diffusivity of a single solute in solution (m^2 s^{-1})
D_p	pore diffusivity (m^2 s^{-1})
D_s	surface diffusivity (m^2 s^{-1})
K	sorption Freundlich constant (g kg^{-1})(g m^{-3})$^{-1/n}$
K_d	distribution coefficient (dm^3 kg)
K_{di}	Weber and Morris intraparticle diffusion rate Weber and Morris (mg g^{-1} min$^{-1/2}$)
K_{li}	rate constant for film diffusion (infinite solution volume condition)
K_L	sorption Langmuir constant (m^3 kg^{-1})
K_{mA}	mass transfer coefficient of species A through the liquid film (m s^{-1})
K_{ow}	octanol/water coefficient
K_s	reaction constant based on surface (m s^{-1})
K_{s1}	pseudo-first-order rate constant (min^{-1})
K_{s2}	pseudo-second-order rate constant (g mg^{-1} min^{-1})
n	Freundlich exponent
q_e	amount of solute sorbed at equilibrium (mg g^{-1})
q_t	amount of solute sorbed at time (t mg g^{-1})
q_m	solid-phase concentration inside particles, mg g^{-1} of bed
r	average particle radius (m)
t	time (min)
X	fractional attainment of equilibrium or extent of solid conversion

Greek letters

ε_P	intraparticle porosity
η	viscosity (g cm^{-1} s^{-1})
ρ_p	particle density (g L^{-1})
τ	tortuosity factor

fact that PAHs are removed from the water rather than being broken down by oxidation or reduction to potentially more dangerous metabolites. Due to the long time scales necessary for full remediation, passive groundwater remediation using PRBs is considered to be more cost-effective than active methods [11–13].

Activated carbon sorption is the best technology available for the control of many organic contaminants in waters. Treatment options may range from a wide variety of activated carbons that differ in pore structure and surface chemistry to the control of one or more chemical compounds and mixtures [14–16]. A large number of PRB sites have been set up in North America and Europe over the last few years that use systems based on sorption rather than degradation. At most of the sites in Europe, GAC has been used as the "reactive" sorbent material in several in situ remediation projects on PAH removal from groundwater [17].

The volume of water that can be properly treated by a certain amount of GAC is limited as the process depends on the specific sorption capacity of the type of GAC used. Therefore, the sorbent must be replaced when contaminant concentrations exceed a given threshold at the reactor/column/barrier outlet. Granular activated carbon has a porous structure that makes solids both macro- and microporous. This makes it possible to control pore sizes and relatively high surface areas (1000–2000 m^2 g^{-1}).

GAC is particularly suitable for the efficient sorption of high molecular weight organic molecules with lipophilic properties, as is the case of PAHs [18–21]. Although GAC has been used for groundwater treatment in numerous cases, few data on equilibrium and kinetic parameters are available in the literature. Thus, the application of these systems in a full-scale PRB (with fixed walls and removable equipment) requires knowledge of the equilibrium and kinetics of the solute extraction processes and their operating behaviour. The determination of the kinetic parameters has two objectives: (i) to approach, as accurately as possible, the real physical chemistry of the solute sorption process and (ii) to obtain empirical or semi-empirical equations for the design of the PRB.

Kinetic PAH sorption data for a given sorbate/sorbent pair are generally scarce. Therefore, it would be desirable to develop a tool capable of predicting the kinetic sorption performance of GAC for aqueous trace PAHs based on fundamental sorbent and sorbate properties. For this purpose, a family of PAHs with two to four rings was evaluated in a set of kinetic sorption tests. This paper describes the PAH extraction kinetics behaviour of GAC. The aim is to determine the kinetic parameters of the PAH sorption process in the conditions expected to be found in ground and industrial wastewater with a PAH content in the range of 0.2–10 mg L^{-1}. The description of the kinetic process was achieved by analysing the kinetic measurements in synthetic solutions.

2. Material and methods

2.1. Reagents and solutions

The GAC sample was provided by Aguas de Levante (Spain). The sample used (F400) was an activated carbon specially tailored for the treatment of organic contaminants, macromolecules, colour, taste and smell. It is an activated carbon with a macroporous volume of 1.5 cm^3 g^{-1} and a BET surface area of 1000 m^2 g^{-1}. It has an ash content of 5% (maximum). A coarse grade of the product was supplied (in a range of 0.5–8 mm). A GAC in the 3–6 mm size range was used for all the experiments.

It was subsequently washed with deionized water several times to remove fines from the sorbent and was dried at 100–120 °C for 48 h. The carbon particles were assumed to be "spheres" whose diameter is given by the arithmetic mean value of the respective mesh sizes.

The PAHs (acenaphthene, anthracene, fluorene, fluoranthene, naphthalene and pyrene) were purchased from Merck and Aldrich Chemical Co. Acetonitrile was purchased from Panreac.

The PAH solutions were prepared from a stock solution of each PAH in acetonitrile. Synthetic solutions were prepared by proper dilution in deionized water. The characteristics of the PAHs and the composition solutions are shown in Table 1.

2.2. PAH analysis

The composition of the aqueous solutions varied depending on the nature of the experiment. PAH content in the aqueous phase was determined by UV–vis Spectrophotometry (Hewlett Packard, model HP-8453). The extent of sorption was calculated from the residual concentration of the PAH in the equilibrated solution. The absorbance values of PAHs, were determined at the following wavelengths: acetonaphthene, 281 nm; anthracene, 358 nm; fluoranthene, 286 nm; fluorene, 261 nm; naphthalene, 266 nm; pyrene, 272 nm.

2.3. Batch kinetics experiments

A standard agitated reactor experimental set-up was used to determine the kinetic data of F400. A wet-sieved F400 fraction of narrow particle size range (3–6 mm) was used.

Dynamic contact between the GAC and the solution was carried out on a mechanical shaker at different shaking speeds to determine the minimum speed above which the kinetics are independent of the degree of agitation and, hence, not influenced by film diffusion. Sorption rates were always measured above this minimum speed. The kinetic analysis was carried out at room temperature (21 ± 1 °C). PAH solutions of 200 cm^3 were put in contact with 0.3 g of sorbent in a 500 cm^3-glass reactor until equilibrium was achieved (400 min). Samples were filtrated through a 0.45 μm filter to eliminate the fines generated during shaking and to avoid interferences in the quantification step. The extent of sorption was determined by measuring the residual amount of sorbate in the liquid. The reproducibility of the results was greater than 95% after three replicates for each experiment.
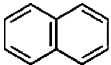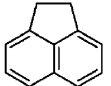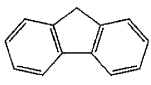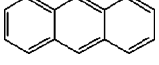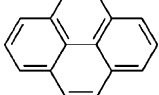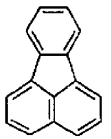
2.4. SEM analysis

A JEOL 3400 Scanning Electron Microscopy with Energy Dispersive System (SEM-EDS) was used to observe the surface morphology of GAC. Prior to analysis, samples were dried in a vacuum oven at room temperature and then gold coated.

3. Results and discussions

3.1. Kinetic sorption models for non-polar organic micropollutants

The sorption of organic micropollutants onto natural and synthetic sorbents has been described as a complex process, in which the properties of the sorbate and the solvent often play a critical role. The sorption process occurs within the boundary layer around the sorbent and proceeds in the liquid-filled pores or along the walls of the pores of the sorbent. The latter two processes are called the external and internal mass transfer steps, respectively.

Table 1
Characteristics of PAHs and composition solutions

PAH	Structure	Solubility 25° (mg dm^{-3})	log K_{ow}	Molar volume (cm^3 mol^{-1})	Concentration range (mg dm^{-3}); % acetonitrile
Naphthalene		30.8	3.4	148	(0–5); (0)
Acenaphthene		4.5	3.9	173	(0–20); (0–10)
Fluorene		2.0	4.2	188	(0–5); (0–10)
Anthracene		0.045	4.6	197	(0–20); (0–40)
Pyrene		0.13	5.2	214	(0–5); (0–20)
Fluoranthene		0.21	5.2	217	(0–10); (0–30)

The sorption of organic micropollutants using GAC, as is the case of other heterogeneous processes between solids and fluids, could be explained through a number of sequential processes that determine the rate of reaction: (a) the diffusion of the solute through the liquid film surrounding the particle (liquid film diffusion control); (b) the diffusion of the solute through the sorbent matrix of the GAC (particle-diffusion control); (c) the chemical reaction with the functional groups attached to the matrix. One of these steps usually offers much greater resistance than the others and may thus be considered as the rate-limiting step of the process [22]. However, when the chemical reaction of a PAH on the sorbent surfaces may be explained as a chemisorption process, it is usually assumed to be too fast to affect the overall sorption rate, unless chemical modifications occur during sorption. Conditions for liquid film diffusion control of the overall sorption rate are well known and are mainly comprised of a low degree of agitation, low solution concentration and small particle size.

The kinetic models selected to describe the solute extraction data are two models widely used for fitting sorption and ion exchange data: the homogeneous particle diffusion model (HPDM) and the shell progressive model (SPM) or the shrinking core model [22,23].

3.1.1. The homogeneous particle diffusion model (HPDM)

In this model, the extraction mechanism involves the diffusion of PAH molecules from the aqueous solution into the sorbent phase through a number of possible resistances. The sorption of the PAH molecules can be rigorously described by Fick's equation. This applies the diffusion of PAH compounds in a quasi-homogeneous media. The sorbent phase controlled diffusion of PAH molecules from an infinite volume of solution into sorbent particle was described by Boyd et al. [24]. As the diffusion rate controls sorption on spherical particles, the solution of the simultaneous set of differential and algebraic equations gives:

$$X(t) = 1 - \frac{6}{\pi^2} \sum_{z=1}^{\infty} \frac{1}{z^2} \exp\left[\frac{-z^2 \pi^2 D_e t}{r^2}\right] \tag{1}$$

where $X(t)$ is the fractional attainment of equilibrium at time t, D_e the effective diffusion coefficient of sorbates in the sorbent phase ($m^2 s^{-1}$), r the radius of the sorbent particle assumed to be spherical (m), and z is an integer.

$X(t)$ values could be calculated by using the following equation:

$$X(t) = \frac{q_t}{q_e} \tag{2}$$

where q_t and q_e are solute loading on the solid phase at time t and when equilibrium is attained (mg g^{-1}), respectively.

Vermeulen's [25] approximation of the Eq. (1) fits the whole range $0 < X(t) < 1$, for sorption on spherical particles:

$$X(t) = \left[1 - \exp\left[-\frac{\pi^2 D_e^2 t}{r^2}\right]\right]^{1/2} \tag{3}$$

This equation could be further simplified to cover most of the data points for calculating effective particle diffusivity by using

the following expression:

$$-\ln(1 - X^2(t)) = 2Kt, \quad \text{where } K = \frac{\pi^2 D_e}{r^2} \tag{4}$$

If liquid film diffusion controls the rate of sorption, the following analogous expression can be used:

$$X(t) = 1 - \exp\left[-\frac{3D_e C}{rC_r}\right] \tag{5}$$

$$-\ln(1 - X(t)) = K_{li}t \quad \text{where } K_{li} = \frac{3D_e C}{rC_r} \tag{6}$$

3.1.2. The shell progressive model (SPM)

The shell progressive or unreacted shrinking core model is a mass transfer model in which the reaction starts at the particle surface, which forms a reacted zone and moves inward at a certain velocity.

In this case, the relationship between the sorption time and the degree of sorption is given by the expressions below [23,26].

(a) When it is controlled by the fluid film:

$$X(t) = \frac{3C_{Ao}K_{mA}}{a_s C_{so}}t \tag{7}$$

(b) When it is controlled by the diffusion though the sorption layer:

$$[3 - 3(1 - X(t))^{2/3} - 2X(t)] = \frac{6D_e C_{Ao}}{a_s^2 C_{so}}t \tag{8}$$

(c) When it is controlled by the chemical reaction:

$$[1 - (1 - X(t))^{1/3}] = \frac{K_s C_{Ao}}{r}t \tag{9}$$

The description of the rate of sorption based on a shell-core mechanism may be valid for species with a high affinity for GAC, which results in quasi-irreversible sorption. Since PAH solutes have a large binding constant on GAC, attempts were made to fit kinetic sorption data to shell–core models.

3.2. Kinetic performance of GAC on PAH extraction from aqueous solutions

The aim of this kinetic study was to find a diffusion model that describes the experimental data. This was in order to determine the rate controlling steps and the kinetic parameters of the mass transfer for each PAH. However, since the data were collected under conditions of minimum film diffusion resistance, the models based on reacted layer diffusion control and chemical reaction control were tested first.

Kinetics measurements in the extraction of PAH with GAC in the range 0.2–10 mg L^{-1} were made. The studied PAH concentration range covered the typically achieved values in contaminated groundwater as described in the literature for remediation projects [12,13].

All experimental data were treated graphically with all the fractional attainment of equilibrium functions $F(X) = f(t)$ defined in Section 3.1 for both the HPDM and SPM models.
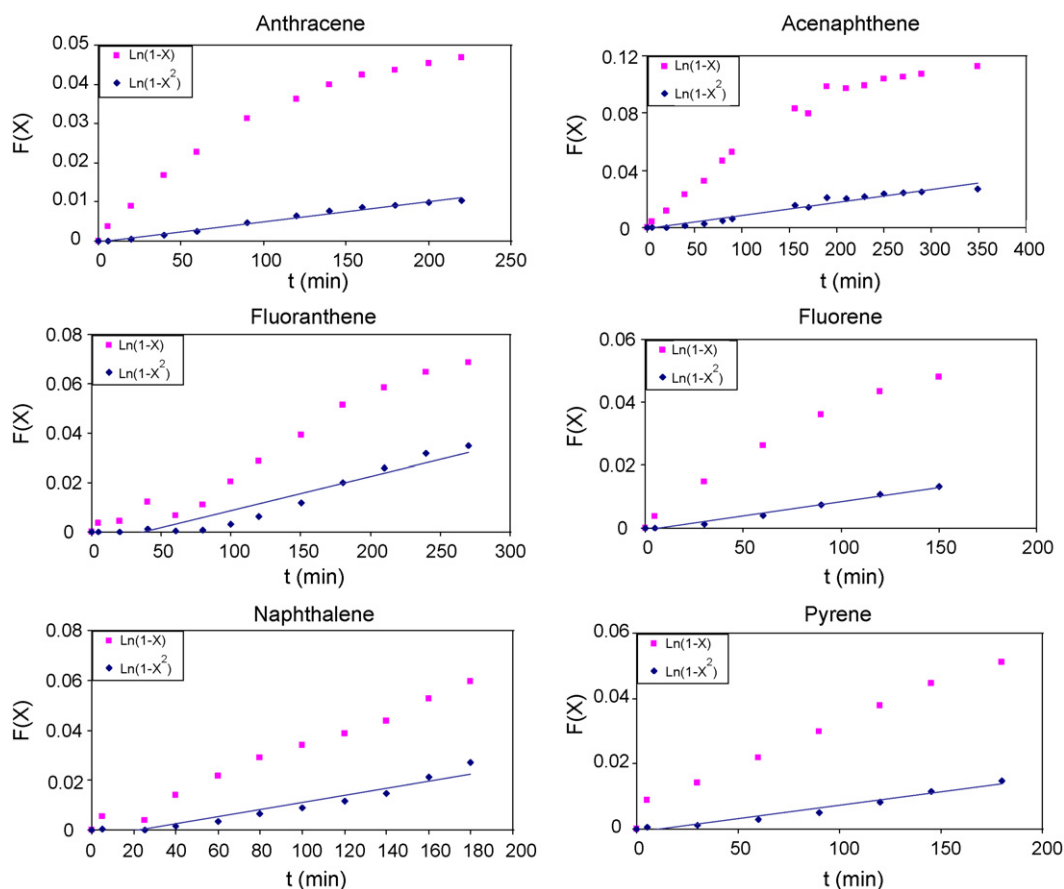
Fig. 1. Test of the kinetic model equations $F(X)$ vs. t defined by the homogenous particle diffusion model for PAH sorption on GAC of bead size 3–6 mm.

Figs. 1 and 2 show the results of the different PAH sorption kinetics in the form of Eqs. (4) and (6) for the HDM model and Eqs. (7)–(9) for the SPM model. It can be observed in Figs. 1 and 2 that chemical reaction and film diffusion control can be discarded as the controlling step since the fit did not give a linear dependence. Both the HPDM and SPM models fit the data satisfactorily in almost the entire range for sorbent-phase diffusion, with some variation in the initial time for some PAHs. An apparent linear relationship could also be obtained for the film diffusion model over a shorter time range.

The results of the linear regression analysis for Eqs. (4) and (8) for the different PAH compounds are summarized in Tables 2 and 3. The straight lines that are obtained in all cases do not pass through the origin as they should because of a slight deviation from linearity near this point. This result can be explained by the fact that at the beginning of the reaction, the thickness of the reacted layer is still very small and thus comparable to that of the liquid film adjacent to the particle. The film resistance to diffusion of the reactant is therefore comparable to the resistance provided by the sorbent outer shell.

The linear correlation coefficients indicate a good fit for both models. The slope values were used to calculate effective diffusion coefficients (D_{eff}) for the different PAHs using Eqs. (4) and (8). These diffusion coefficients are in fact a measure of the mean inter-diffusion coefficient of the PAH molecules involved in the sorption process. Scarce data for the sorbent/solute pairs have been found in the literature. the sorption process. Scarce data for the sorbent/solutes couples have been found on the literature.

Table 2
Lineal regression analysis of functions $-\ln(1 - X^2)$ vs. time (t) (homogeneous diffusion model)

PAH	$F(X) = f(t)$ intercept	$F(X) = f(t)$ slope (min^{-1})	r^2	D_s (m^2 s^{-1})
Naphthalene	-4.62×10^{-4}	1.93×10^{-5}	0.93	3.66×10^{-14}
Acenaphthene	-4.01×10^{-4}	3.85×10^{-5}	0.96	7.31×10^{-14}
Fluorene	-1.16×10^{-4}	1.53×10^{-5}	0.99	2.90×10^{-14}
Anthracene	-4.88×10^{-5}	1.04×10^{-5}	0.99	1.97×10^{-14}
Pyrene	-1.49×10^{-4}	1.36×10^{-5}	0.97	2.58×10^{-14}
Fluoranthene	-6.40×10^{-4}	1.72×10^{-5}	0.91	3.28×10^{-14}

Table 3
Lineal regression analysis of functions $(3 - 3(1 - X)^{2/3} - 2X)$ vs. time (t) (shell progressive model)

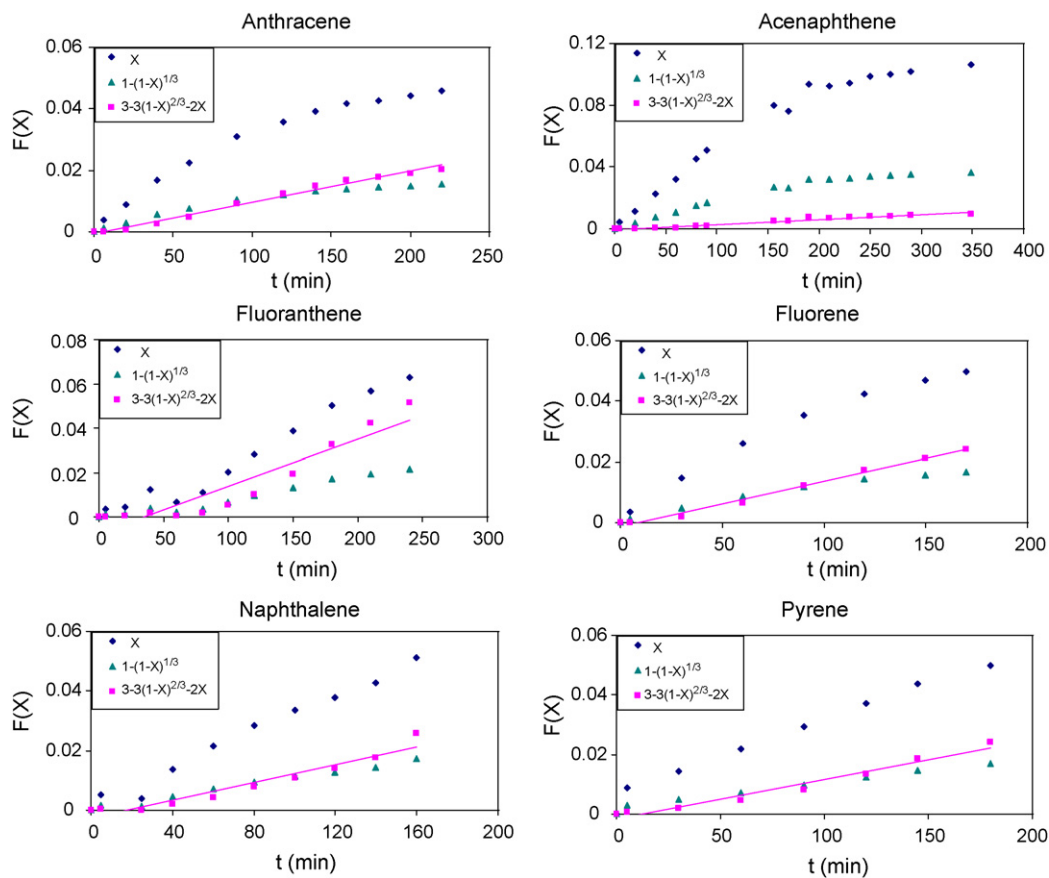| PAH	$F(X) = f(t)$ intercept	$F(X) = f(t)$ slope (min^{-1})	r^2	D_e (m^2 s^{-1})
Naphthalene	-1.60×10^{-4}	6.59×10^{-6}	0.93	3.08×10^{-14}
Acenaphthene	-1.49×10^{-4}	1.34×10^{-5}	0.96	7.53×10^{-14}
Fluorene	-4.00×10^{-5}	5.19×10^{-6}	0.99	2.89×10^{-14}
Anthracene	-1.74×10^{-5}	3.52×10^{-6}	0.99	2.09×10^{-14}
Pyrene	-5.17×10^{-5}	4.62×10^{-6}	0.97	2.47×10^{-14}
Fluoranthene	-2.20×10^{-4}	5.90×10^{-6}	0.91	3.12×10^{-14}

Fig. 2. Test of the kinetic model equations $F(X)$ vs. t defined by the shell progressive model for PAH sorption on GAC of bead size 3–6 mm.

3.3. Effect of solute on intraparticle diffusion

The effective application of GAC requires a detailed knowledge of their structural (geometric) and surface heterogeneities. Aqueous phase sorption onto carbonaceous sorbents is influenced by several factors, in particular the chemical composition of the carbon surface, the pore size distribution, and the internal surface area. The size, shape and physic-chemical properties of molecules occurring in source waters are also important.

In a previous study, the sorption equilibrium data were determined using three isotherm models: the Freundlich, Langmuir and Redlich–Peterson models. Table 4 shows the isotherm parameters obtained. The sorption of hydrophobic compounds such as PAHs from the aqueous phase increases as the solubility of the compound decreases (or as the octanol–water partition coefficient K_{ow} increases). The sorptive behaviour of PAHs appears to be dominated by this hydrophobic characteristic. The sorption equilibrium constant, e.g. the Langmuir isotherm coefficient ($\log K_L$), follows a linear dependence with the octanol–water partition coefficient ($\log K_{ow}$), as can be seen in Fig. 3. The affinity of a PAH is correlated to the hydrophobicity of its non-polar moiety. Fig. 3 shows that the octanol–water partition coefficient (K_{ow}) of the PAH family of compounds under evaluation is a representative measure of the non-polar moiety's hydrophobicity. The sequence of sorption affinity, i.e. pyrene ≈ fluoranthene > anthracene > fluorine > acenaphthene > naphthalene, is in accordance with the increase in hydrophobic-
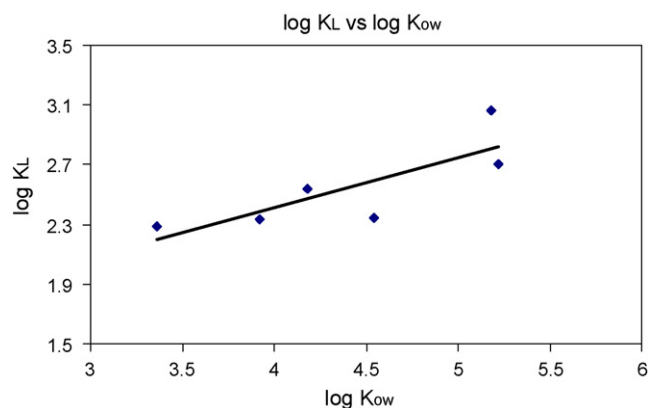

Fig. 3. Comparison of the Langmuir isotherm coefficient K_L with octanol–water coefficient $\log K_{ow}$ of six PAH onto GAC.

ity or the octanol–water partition coefficient of the non-polar moiety of the aromatic rings [27].

Similar behaviour was observed when the pseudo-first-order constant (K_{s1}) and pseudo-second-order (K_{s2}) were correlated with octanol water coefficient [28]. The kinetic parameters of three models (pseudo-first-order, pseudo-second-order and Elovich) are collected in Table 5.

From a phenomenological point of view, this observation implies that a target PAH with a greater K_{ow} will result in a lower D_{eff} value and will hence give rise to a longer or more diffuse mass transfer zone during a fixed bed filter run.

Table 4
Langmuir, Freundlich and Redlich–Peterson isotherms parameters for six PAH onto granular activated carbon

PAH/isotherm	Langmuir		Freundlich		Redlich–Peterson		
	K_L (m^3 kg^{-1})	q_m (g kg^{-1})	K (g kg^{-1})(m^3 g^{-1})$^{-1/n}$	n	A (dm^3 g^{-1})	B (dm^3 mg^{-1})	g
Naphthalene	192	140	30.8	2.9	121	2.6	0.7
Acenaphthene	216	111	34.6	3.8	160	1.7	0.9
Fluorene	343	145	39.2	2.7	150	2.6	0.7
Anthracene	223	232	40.2	3.0	280	5.5	0.6
Pyrene	1157	109	63.9	8.4	170	1.6	1.0
Fluoranthene	505	93	29.5	4.2	54	1.6	0.7

Table 5
Parameters of pseudo-first-order, pseudo-second-order and Elovich models for PAHs sorption process on activated carbon

Model	Naphthalene	Acenaphthene	Fluorene	Anthracene	Pyrene	Fluoranthene
Pseudo-first-order						
K_{s1} (min^{-1})	1.2×10^{-2}	9.9×10^{-3}	2.1×10^{-2}	1.5×10^{-2}	1.4×10^{-2}	1.1×10^{-2}
q_e (mg dm^{-3})	12.12	15.22	10.59	14.60	7.11	9.88
R^2	0.87	0.97	0.92	0.93	0.91	0.90
Pseudo-second-order						
K_{s2} (mg min^{-1})	1.7×10^{-5}	3.2×10^{-4}	5.7×10^{-4}	5.9×10^{-4}	3.1×10^{-4}	1.4×10^{-4}
q_e (g kg^{-1})	15.19	20.81	12.90	15.50	12.89	18.76
R^2	0.95	0.97	0.99	0.99	0.98	0.70
Elovich						
b (g mg^{-1})	2.5×10^{-1}	3.5×10^{-1}	4.8×10^{-1}	2.8×10^{-1}	4.2×10^{-1}	5.7×10^{-1}
a (g mg^{-1} min^{-1})	0.22	0.30	0.34	0.40	0.12	0.12
R^2	0.84	0.93	0.95	0.97	0.96	0.76

This relationship could be used as log K_{ow} for the estimation of PAH sorption kinetics as a function of measured physical properties.

It could be conjectured that the most important step in a given groundwater procedure by the application of GAC will largely depend on the size of the organic compounds to be removed. Moreover, a breakdown of the approximate sizes helps to explain the fact that mesopores may be as important as micropores when high molecular-weight compounds are present. It is clear that a large micropore volume (high surface area) results in the efficient removal of small molecules. However, water treatment applications that deal with larger molecules such as PAHs, which thus includes mesopores and macropores, may be also important [29,30].

3.4. Analysis of intraparticle diffusivity mechanisms

The scanning electron microscopy examination of the F400, as presented in Fig. 4, shows a heterogeneous phase material. The particle size diameter is approximately 600–750 nm for the GAC; thus large pores are created that will enable the rapid diffusion of solutes. Fig. 4 shows that micropores and macropores have an irregular surface in comparison to hypercrosslinked polymeric sorbents with similar surface areas [27]. The F400 contains micropores 0.6–1.4 nm in diameter and macropores whose average diameter is 100–200 nm. Pore volume accounts for 20% of macro- and mesopores, which indicates that the GAC sample analysed has a significant number of meso- and macropores in comparison with the number of fine pores.

The sorption of PAHs onto a porous sorbent such as GAC goes through three consecutive stages. The first stage is assumed to occur rapidly and does not form a rate-limiting stage in the sorption of organic compounds on activated carbons. It is proposed that the main resistance to mass transfer occurs solely in the second stage, during the movement or diffusion of the PAH in the internal structure of the sorbent. It is suggested that the pore structure of the sorbent particles used in the process consists of macropores, transitional pores (or mesopores) and micropores. The transitional pores are instrumental in the transport of sorbate
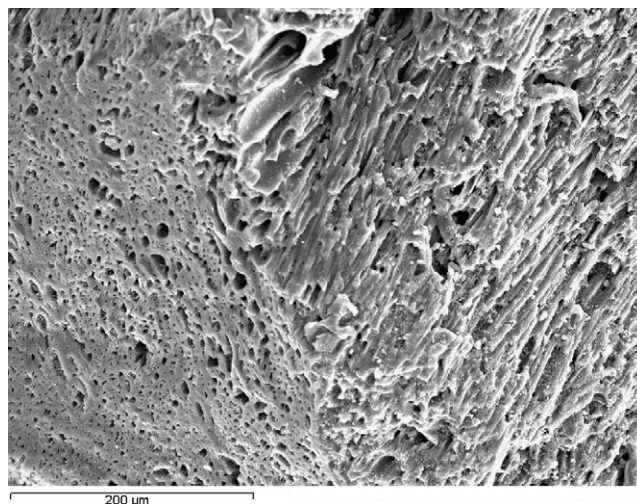

Fig. 4. Scanning electron micrographs of the activated carbon F400 bead internal area.
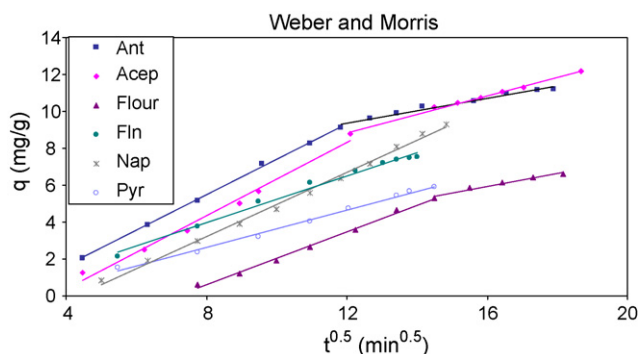
Fig. 5. Weber and Morris intra-particle diffusion plots for removal for PAH sorption on GAC of bead size 3–6 mm.

Table 6
Change of slopes (K_{di}) from Weber and Morris equation obtained for activated carbon F400

PAH	K_{di} (mg g^{-1} min^{-1})			
	K_{di1}	r_1^2	K_{di2}	r_2^2
Naphthalene	0.76	0.96		
Acenaphthene	0.99	0.99	0.42	0.92
Fluorene	0.62	0.99		
Anthracene	0.96	0.99	0.30	0.99
Pyrene	0.46	0.98		
Fluoranthene	0.72	0.99	0.35	0.97

molecules to the micropores. Most molecular sorption pores will incorporate diffusive mass transfer based on a pore, surface or pore-surface diffusion control mechanism. The interpretation of the overall sorption behaviour in terms of the true diffusivity and equilibrium properties is not always straightforward. However, an apparent diffusion coefficient can be derived by fitting the experimental sorption data obtained.

The mass transfer kinetics of PAHs on GAC is relatively slow. Theoretically, the solute transport inside a macroporous sorbent particle occurs in parallel through both the pore and solid phases. This parallel solute transport mechanism has formed the basis of several intraparticle diffusion models for macroporous particles [18,31]. The intraparticle diffusion model developed by Weber and Morris [32] could be used as a first approach for describing sorption processes on the GAC. The mathematical dependence of uptake $q(t)$ of sorbates (PAH) on $t^{1/2}$ is obtained if the sorption process is considered to be influenced by diffusion in the spherical sorbent and by convective diffusion in the sorbate solution. This dependence is given by the following equation:

$$q_t = K_{di}\sqrt{t} + A \tag{10}$$

where k_{di} is the intraparticle diffusion rate constant (mg g^{-1} min$^{-1/2}$) and A (mg g^{-1}) is a constant that gives an indication of the thickness of the boundary layer, i.e. the higher the value of A, the greater the boundary layer effect.

It is assumed that the external resistance to mass transfer surrounding the particles is significant only in the early stages of sorption. This can be seen in the initially steeper linear. The second linear portion is the gradual sorption stage in which intraparticle diffusion dominates.

If the Weber–Morris [32] plot of q_t versus $t^{1/2}$ gives a straight line, this means that the sorption process is only controlled by intraparticle diffusion. However, two or more steps influence the sorption process if the data exhibit multi-linear plots. Fig. 5 plots the mass of PAHs sorbed per unit mass of sorbent versus $t^{1/2}$ for the GAC sorbent. The external resistance was discarded and two straight lines were expected for each PAH. The first line depicts macropore diffusion and the second represents micropore diffusion until equilibrium was achieved. However, no clear separation of these two processes was detected for all the PAHs (Fig. 5). Three PAHs (anthracene, acenaphthene

and fluoranthene) gave a single straight line, which indicates that intraparticle diffusion acts as the controlling step for PAH sorption on the GAC.

The intraparticle diffusion constants can be calculated using Eq. (9). Table 6 shows the intraparticle diffusion constants (K_{di1}, K_{di2}) and the correlation coefficient (r^2). From Table 6, it can be seen that the order of the sorption rate was higher in the first stage (K_{di1}) than in the second stage (K_{di2}) for three PAHs (fluorene, naphthalene and pyrene), for which there was a significant change in the slope. Initially, the PAHs are sorbed by the external macropore structure of the F400 particles, so the sorption rate was very high. When the sorption of the macroporous structure reached saturation, the PAH molecules diffused in the internal surface pores within the particle (micropore structure) and then were sorbed by the internal surface of the carbonaceous particles. When the PAH molecules diffused in the micropores of the particle, the diffusion resistance increased, which caused the diffusion rate to decrease. When the PAH concentration in the solution was decreased, the diffusion rate became lower and the diffusion processes reached the final equilibrium stage. Thus, the changes in K_{di1} and K_{di2} could be attributed to the sorption stages of the external and internal surfaces and the equilibrium approach, respectively. The existence of these macropore and micropore diffusion processes was described by Terzyc and Gauden [33] in their study on the sorption properties of GAC in dissolved organic matter.

3.5. Pore and surface diffusion coefficients

Homogeneous and heterogeneous intraparticle diffusion models (with two or more steps) have been described in the literature [32,33]. The pore diffusion model is probably the simplest, and has been widely used for many porous sorbents. Another simple model is the surface diffusion model, which is sometimes called the solid diffusion model because each particle is assumed to be a homogeneous solid phase. However, the real GAC structure is not always homogeneous as revealed by SEM analysis. Several heterogeneous models have been considered to model diffusion in this structure based on a two-step diffusion process through macropores and micropores. The heterogeneous model is probably the more realistic of these two diffusion models as it takes into account both pore diffusion and surface diffusion with intrinsic pore and surface diffusivities [18,34]. By considering these phenomena, the transport of a PAH in a single porous

particle may be written as:

$$\varepsilon_p \frac{\partial C_{PAH}}{\partial t} + \rho_p(1-\varepsilon_p)\frac{\partial q_{PAH}}{\partial t} = \varepsilon_p D_p \left(\frac{\partial^2 C_{PAH}}{\partial^2 r^2} + \frac{2}{r}\frac{\partial C_{PAH}}{\partial r}\right)$$

$$+ \rho_p(1-\varepsilon_p)D_s\left(\frac{\partial^2 q_{PAH}}{\partial^2 r^2} + \frac{2}{r}\frac{\partial q_{PAH}}{\partial r}\right) \quad (11)$$

where the first terms on either side represent the contributions of pore diffusion, the second terms on either side correspond to solid phase diffusion, ε_P is the internal porosity of the sorbent, ρ_p is the true density of the porous support, D_p and D_s are the pore and surface diffusion coefficients, respectively, C_{PAH} is the liquid-phase concentration of PAH per unit volume of liquid phase and q_{PAH} is the solid-phase concentration per unit mass of the sorbent.

Taking into account the sorption equilibrium of the PAH described by the Langmuir isotherm gives:

$$q_{PAH} = \frac{K_{L(PAH)}q_m C_{PAH}}{1 + K_{L(PAH)}C_{PAH}} \quad (12)$$

which could be simplified for the low PAH concentration range where $1 \gg K_{L(PAH)}C_{PAH}$ to:

$$q_{PAH} = K_{L(PAH)}q_m C_{PAH} \quad (13)$$

Hence,

$$\frac{\partial q_{PAH}}{\partial t} = K_{L(PAH)}q_m \frac{\partial C_{PAH}}{\partial t} \quad \text{and} \quad \frac{\partial^2 q_{PAH}}{\partial^2 r^2}$$

$$= K_{L(PAH)}q_m \frac{\partial^2 C_{PAH}}{\partial^2 r^2} \quad (14)$$

which may be rearranged as:

$$\frac{\partial q_{PAH}}{\partial t} = \frac{\varepsilon_p D_p + K_{L(PAH)}q_m \rho_p(1-\varepsilon_p)D_s}{\varepsilon_p + K_{L(PAH)}q_m \rho_p(1-\varepsilon_p)}$$

$$\times \left(\frac{\partial^2 q_{PAH}}{\partial^2 r^2} + \frac{2}{r}\frac{\partial q_{PAH}}{\partial r}\right)$$

$$= D_{eff}\left(\frac{\partial^2 q_{PAH}}{\partial^2 r^2} + \frac{2}{r}\frac{\partial q_{PAH}}{\partial r}\right) \quad (15)$$

where the effective intraparticle diffusivity (D_{eff}) is:

$$D_{eff} = \frac{\varepsilon_p D_p + K_{L(PAH)}q_m \rho_p(1-\varepsilon_p)D_s}{\varepsilon_p + K_{L(PAH)}q_m \rho_p(1-\varepsilon_p)} \quad (16)$$

For a favourable sorption process, as is the case of PAH onto GAC F400, the following applies:

$$\varepsilon_p << K_{L(PAH)}q_m \rho_p(1-\varepsilon_p) \quad (17)$$

Thus,

$$D_{eff} = D_s + \frac{\varepsilon_p D_p}{K_{L(PAH)}q_m \rho_p(1-\varepsilon_p)} \quad (18)$$

The pore diffusion coefficient could be estimated from the diffusion coefficients in water (D_m) by using the following equation:

$$D_p = \frac{D_m \varepsilon_p}{\tau} \quad (19)$$

where the tortuosity factor τ of the GAC particles is given by:

$$\tau = \frac{(2-\varepsilon_p)^2}{\varepsilon_p} \quad (20)$$

Thus,

$$D_{eff} = D_s + \frac{\varepsilon_p^2 D_m}{K_{d(PAH)}\rho_p \tau(1-\varepsilon_p)} \quad (21)$$

The molecular diffusion coefficient D_m was calculated according to the Wilke–Chang equation as follows [35]:

$$D_m = 7.4 \times 10^{-8}T\frac{(\alpha_A M_S)^{0.5}}{\eta V_A^{0.6}} \quad (22)$$

where T is the absolute temperature (K), V_A is the molar volume of the solute at its normal boiling point, M_S is the molecular weight of the fluid, η is the fluid viscosity (cp), and α_A, the association factor for the fluid that accounts for solute–solvent interactions, was 2.6.

In this preliminary approach, Eq. (18) was used to estimate the surface diffusion coefficients of PAHs on the micropore structure of GAC. Previously determined D_{eff} values (see Tables 2 and 3) for the two models (HPDM and SPM) were used to determine the surface diffusion coefficient. This heterogeneous model is appropriate for the direct fitting of data and can be used as a preliminary method for estimating surface diffusivity [18]. As discussed above (Section 3.3), there is clear evidence that pore diffusion is not the only important mechanism in the sorption process and that surface diffusion is an important mechanism in this system, especially in the second stage of the sorption process (Fig. 5). The surface diffusion coefficients (D_s) based on the D_{eff} values calculated for the HPDM and SPM models are shown in Table 7.

Scarce data of the sorption of PAH onto GAC could be found in the literature. In most cases, the data available were chemical interpretations. If this work is compared with sorption data on PAH removal by hypercrosslinked polymeric resins, the range of the apparent surface diffusivities are very close to the result reported for this specific sorbent [27,36]. The apparent surface diffusivity coefficients were compared (Table 8) with measured values of functionalized aromatic hydrocarbons such as phenol, *p*-bromophenol, *p*-nitrophenol, *p*-toluenesulphonate and dodecylbenzenesulphonate [37–42]. As a general rule, values of D_s

Table 7
Surface diffusion coefficients values obtained by the shell progressive model and the homogeneous diffusion model for activated carbon F400

PAH	Model			
	Shell progressive model (m^2 s^{-1})		Homogeneous diffusion model (m^2 s^{-1})	
	D_{eff}	D_s (calc.)	D_{eff}	D_s (calc.)
Anthracene	2.1×10^{-14}	1.8×10^{-14}	2.0×10^{-14}	1.6×10^{-14}
Acenaphthene	7.5×10^{-14}	6.8×10^{-14}	7.3×10^{-14}	6.6×10^{-14}
Fluoranthene	3.1×10^{-14}	2.7×10^{-14}	3.3×10^{-14}	2.9×10^{-14}
Fluorene	2.9×10^{-14}	2.5×10^{-14}	2.9×10^{-14}	2.6×10^{-14}
Naphthalene	3.1×10^{-14}	2.3×10^{-14}	3.7×10^{-14}	2.9×10^{-14}
Pyrene	2.5×10^{-14}	2.3×10^{-14}	2.6×10^{-14}	2.4×10^{-14}

Table 8
Surface diffusion coefficients reported for different organic solutes on activated carbon F400

Organic solutes	D_s (m^2 s^{-1})
Phenol	1.2×10^{-13}
2-Dodecil-benzene-sulfonate	9.9×10^{-14}
p-Tolueno-sulfonate	6.2×10^{-13}
p-Bromo-phenol	2.2×10^{-13}
PCP	6.3×10^{-13}
PNP	3.8×10^{-13}

were in the same order as the measured values of the PAH evaluated. Ahn et al. [43] reported surface diffusion coefficients for phenanthrene and pyrene on coarse activated carbon using a branched pore kinetic model, the values of which were 2×10^{-15} and 3×10^{-16} m^2 s^{-1}, respectively.

4. Conclusions

HPDM and SPM models can be used in the study of PAH removal by GAC. The results obtained in this work on the kinetic sorption of PAH from aqueous solutions indicated that the rate-determining step of PAH extraction is the sorbent-phase diffusion. Both the HPDM and SPM models allow a mean or average intraparticle diffusion coefficient to be calculated in the case of high levels of PAH and the mass transfer coefficients for the low range of PAH concentrations, which provide an insight into the diffusion mechanism and a parameter for subsequent design calculations. Fick's law and the shell progressive mechanisms represent good general approaches to the kinetics of PAH extraction on granular activated carbon.

The kinetic parameters obtained (surface diffusion) for the F400 were in the same order of magnitude as those measured by other authors for F400 when it is used in the sorption of organic micropollutants (aromatic hydrocarbons, phenolic compounds and dyes). A comparison of published data on kinetic parameters in the form of surface diffusion coefficients with measured data were in the order of 10^{-13}–10^{-14} m^2 s^{-1}.

References

[1] A. Kaschl, S. Heidrich, S. Weiz, H. Rügner, G. Teutsch, Set of criteria for the suitable assesment of MNA as a site remediation measure as input of the IMS, WELCOME project, 2003.

[2] USEPA, Presumptive Remedies: Technology Selection Guide for Wood Treated Sites, Office of Solid Waste and Emergency response EPA540-F-93-020, 1993.

[3] USEPA, Test methods for evaluating solid waste physical/chemical methods including final update III, Office of Solid Waste and United States Department of Commerce PB97-501928, 1997.

[4] USEPA, Understanding the safe drinking water act, Office of Water EPA 816-F-02-013, 2002.

[5] B.L. Hall, T.E. Lachmar, R.R. Dupont, Field monitoring and performance evaluation of an in situ air sparging system at a gasoline-contaminated site, J. Hazard. Mater. 74 (2000) 165–186.

[6] C.L. Chun, J.-J. Lee, J.-W. Park, Solubilization of PAH mixtures by three different anionic surfactants, Environ. Pollut. 118 (2002) 307–313.

[7] N. Kulik, A. Goi, M. Trapido, T. Tuhkanen, Degradation of polycyclic aromatic hydrocarbons by combined chemical pre-oxidation and bioremediation in creosote contaminated soil, J. Environ. Manage. 78 (2006) 382–391.

[8] M.A. Engwall, J.J. Pignatello, D. Grasso, Degradation and detoxification of wood preservatives creosote and pentachlorophenol in water by the photo-Fenton reaction, Water Res. 33 (1999) 1151–1158.

[9] F.-G. Simon, T. Meggyes, Removal of organic and inorganic pollutants from groundwater using permeable reactive barriers, Land Contam. Reclamation 8 (2000) 103–116.

[10] V. Birke, H. Burmeier, A. Dahmke, M. Ebert, The German permeable reactive barrier (PRB) network "Rubin": temporary overall results and lessons learned after five years of work, in: 9th International FZK/TNO Conference on Soil-Water Systems, 2005.

[11] H. Schad, Perfomance of a full scale PRB in Germany: The Karlsruhe funnel and gate system, in: 9th International FZK/TNO Conference on Soil-Water Systems, 2005.

[12] K.E. Roehl, T. Meggyes, F.G. Simon, D.I. Stewart, Austria Case Study Long Term performance of Permeable Reactive Barriers, 7, Elsevier, 2005.

[13] L. Diels, L. Bastiaens, S. O'Hannessin, J.L. Cortina, P.J. Alvarez, M. Ebert, H. Schad, Permeable Reactive Barriers: a multidisciplinary approach of a new emerging sustainable groundwater treatment technology in 8th International FZK/TNO conference on Soil-Water systems, 2003.

[14] R.M. Kalin, Engineered passive bioreactive barriers: risk-managing the legacy of industrial soil and groundwater pollution, Curr. Opin. Microbiol. 7 (2004) 227–238.

[15] R. Hopman, M.A. Meerkerk, W.G. Wiegers, J.C. Kruithof, The prediction and optimization of pesticide removal by GAC-filtration, Water Supply 12 (1994) 197–207.

[16] A.B. Jusoh, M.J.M.M. Noor, S.B. Piow, Model studies on granular activated carbon adsorption in fixed bed filtration, Water Sci. Technol. 46 (2002) 127–135.

[17] D.R.U. Knappe, V.L. Snoeyink, P. Roche, M.J. Prados, M.-M. Bourbigot, Atrazine removal by preloaded GAC: utilities can use predictions of remaining GAC life to develop a GAC regeneration of replacement schedule, J. Am. Water Works Assoc. 91 (1999) 97–109.

[18] S.D. Faust, O.M. Aly, Chemistry of Water Treatment, second ed., Ann Arabor Press, MI, 1998.

[19] W.J. Weber, S. Liang, A dual particle-diffusion model for porous adsorbents in fixed beds, Environ. Progress 2 (1983) 167–175.

[20] L. Li, P.A. Quinlivan, D.R.U. Knappe, Predicting adsorption isotherms for aqueous organic micropollutants from activated carbon and pollutant properties, Environ. Sci. Technol. 39 (2005) 3393–3400.

[21] H. Jankowska, A. Swiatkoswski, J. Choma, Active Carbon, Ellis Horword Series in Physical Chemistry, England, 1991.

[22] L. Liberti, R. Passino, in: J.A. Marinsky, Y. Marcus (Eds.), Ion Exchange and Solvent Extraction, vol. 7, Marcel Dekker, Inc., New York, 1977 (Chapter 3).

[23] F. Helfferich, Ion Exchange, Mc Graw-Hill, New York, 1962.

[24] G.E. Boyd, A.W. Adamson, L.S. Meyers, The exchange adsorption of ions from aqueous solutions by organic zeolites. III. Performance of deep adsorbent beds under non-equilibrium conditions, J. Am. Chem. Soc. 69 (1947) 2849–2859.

[25] T. Vermeulen, Theory for irreversible and constant-pattern solid diffusion, Industrial Eng. Chem. 45 (1953) 1664–1670.

[26] G. Schmuckler, S. Golstein, in: J.A. Marinsky, Y. Marcus (Eds.), Ion Exchange and Solvent Extraction, vol. 7, Marcel Dekker, Inc., New York, 1977 (Chapter 1).

[27] C. Valderrama, J.L. Cortina, A. Farràn, X. Gamisans, C. Lao, Evaluation of polyaromatic hydrocarbons removal from groundwater by using activated

carbon and hyper-cross-linked macroporous polymer (Macronet MN200), submitted for publication.

[28] C. Valderrama, J.L. Cortina, A. Farran, X. Gamisans, C. Lao, Kinetics of sorption of polyaromatic hydrocarbons onto granular activated carbon and Macronet hyper-cross-linked polymers (MN200), J. Colloid Interface Sci. 310 (2007) 35–46.

[29] S.J. Gregg, K.S.W. Sing, Adsorption Surface Area and Porosoty, second ed., Academic Press, New York, 1992.

[30] Q. Lu, G.A. Soria, The role of adsorbent pore size distribution in multicomponent adsorption on activated carbon, Carbon 42 (2004) 3133–3142.

[31] H. Yoshida, T. Kataoka, S. Ikeda, Intraparticle mass transfer in bidispersed porous ion exchanger. Part I: isotopic ion exchange, Can. J. Chem. Eng. 63 (1985) 422–429.

[32] W.J. Weber, J.C. Morris, Kinetics of adsorption on carbon solution, J. San. Eng. Div. ASCE 89 (1963) 31–59.

[33] A.P. Terzyc, P.A. Gauden, The simple procedure of the calculation of diffusion coefficient for adsorption on spherical and cylindrical adsorbent particles–experimental verification, J. Colloid Interface Sci. 249 (2002) 256–261.

[34] J.-H. Koh, N.-H.L. Wang, P.C. Wankat, Ion exchange of phenylalanine in fluidized/expanded beds, Ind. Eng. Chem. Res. 34 (1995) 2700–2711.

[35] C.R. Wilke, P.I.N. Chang, Correlation of diffusion coefficients in dilute solutions, AIChE J. 1 (1955) 264–270.

[36] M.H. Tai, B. Saha, M. Streat, Characterization and sorption performance of a Hypersol-Macronet polymer and an activated carbon, React. Funct. Polym. 41 (1999) 149–161.

[37] B.M. Van Vliet, W.J. Weber Jr., H. Hozumi, Modeling and prediction of specific compound adsorption by activated carbon and synthetic adsorbents, Water Res. 14 (1980) 1719–1728.

[38] P. Cañizares, M. Carmona, O. Baraza, A. Delgado, M.A. Rodrigo, Adsorption equilibrium of phenol onto chemically modified activated carbon F400, J. Hazard. Mater. 131 (2006) 243–248.

[39] M. Otero, M. Zabkova, A.E. Rodrigues, Adsorptive purification of phenol wastewaters: Experimental basis and operation of a parametric pumping unit, Chem. Eng. J. 110 (2005) 101–111.

[40] P. Chingombe, B. Saha, R.J. Wakeman, Sorption of atrazine on conventional and surface modified activated carbons, J. Colloid Interface Sci. 302 (2006) 408–416.

[41] P. Chingombe, B. Saha, R.J. Wakeman, Effect of surface modification of an engineered activated carbon on the sorption of 2,4-dichlorophenoxy acetic acid and benazolin from water, J. Colloid Interface Sci. 297 (2006) 434–442.

[42] S.D. Faust, O.M. Aly, Adsorption Processes for Water Treatment, Butterworth Publishers, Stoneham, USA, 1987.

[43] S. Ahn, D. Werner, H.K. Karapanagioti, D.R. Mcglothlin, R.N. Zare, R.G. Luthy, Phenanthrene and Pyrene Sorption and Intraparticle Diffusion in Polyoxymethylene, Coke, and Activated Carbon, Environ. Sci. Technol. 39 (2005) 6516–6526.